# Mineralogy and Geochemistry of the Parachute Creek Member of the Green River Formation, Piceance Basin, Colorado, U.S.A.*

**Ariel Malicse[1]**

Search and Discovery Article #50507 (2011)
Posted October 31, 2011

*Adapted from extended abstract prepared in conjunction with poster presentation at AAPG International Conference and Exhibition, Milan, Italy, October 23-26, 2011

[1]SEPCO –UAX/N/TE; Esra Inan, SIEP-USEINO (ariel.malicse@shell.com)

## Abstract

The study describes the Colorado oil shale using core samples in the Piceance Basin, Colorado, U.S.A. (Figures 1 and 2). The Parachute Creek Member consists of mineral zones that reflect the chemical conditions prevailing in the ancient lake (Figures 3, 4, and 5). The mineral zones identified are (Figures 6, 7, and 8): 1) calcite-analcime zone, 2) illite zone, and 3) dawsonite-saline zone.

The calcite-analcime zone is a high TOC interval characterized by high amounts of calcite and analcime (Figures 9 and 10) but low amounts of quartz and potassium feldspar. Albite increases with depth in this zone. The underlying illite zone is a relatively lean, low TOC interval. This zone is characterized by interbedded brecciated and non-brecciated beds. The mineralogy is characterized by high amounts of illite (Figure 11), potassium feldspar, albite, and pyrite; analcime and dawsonite are absent. The illite zone contains anomalously high amounts of Fe, Cr, Zr, and several chalcophile trace elements.

The illite zone marks a major stratigraphic change from the underlying dawsonite-saline zone. Lake conditions were marked by long periods of increased stream runoffs followed by periods of relatively high salinity (up to gypsum saturation). Periods of increased runoff are characterized by lean dolomicrite with detrital illite, whereas, periods of higher salinity are characterized by more organic-rich strata with gypsum pseudomorphs. The abundance of pyrite (Figure 12) and metals can be correlated to the mobility of metal-bearing particulates in relation to the redox conditions in the lake column.

The dawsonite-saline zone is a high TOC interval distinguished by the abundance of dawsonite, nahcolite and quartz. Potassium feldspar and albite (Figure 13) are common; the abundance of albite and dawsonite (Figure 14) are inversely correlated. Vugs lined by pyrite are common.

The kerogen content, mineralogy, and elemental abundances in each mineral zone were strongly influenced by the Eh-pH, salinity, and $PCO_2$ in the ancient lake (Figures 15, 16, and 17). For example, minerals in the calcite-analcime zone reflect stratified meromictic lake with low $PCO_2$, which precluded the precipitation of nahcolite (Figure 18) and dawsonite. The buildup of high $PCO_2$ was prevented by the periodic overturning of the water column.


## Acknowledgements

This study was supervised by Alan Kornacki. Shell SURE Organization funded and approved released of this part of the study. Shell SURE Pyrolysis team provided the XRD and XRF data; whereas, the geologic map and cross-sections were provided by Mark Picha and Jerry Daub.


## References


Cole, R.D., G.J. Daub, and L.K. Weston, 1995, Review of Geology, mineral resources and ground water of Green River Formation, north-central Piceance Creek Basin, Colorado in the Green River Formation, *in* Piceance Creek and Eastern Uinta basins: Grand Junction Geological Society, Grand Junction, Colorado, USA, p. 63-82.

Eugster, H.P., and L.A. Hardie, 1978, Saline lakes, *in* A. Lerman (Ed.), Lakes-Chemistry, Geology, Physics: Springer-Verlag, New York, USA, p. 237-293.

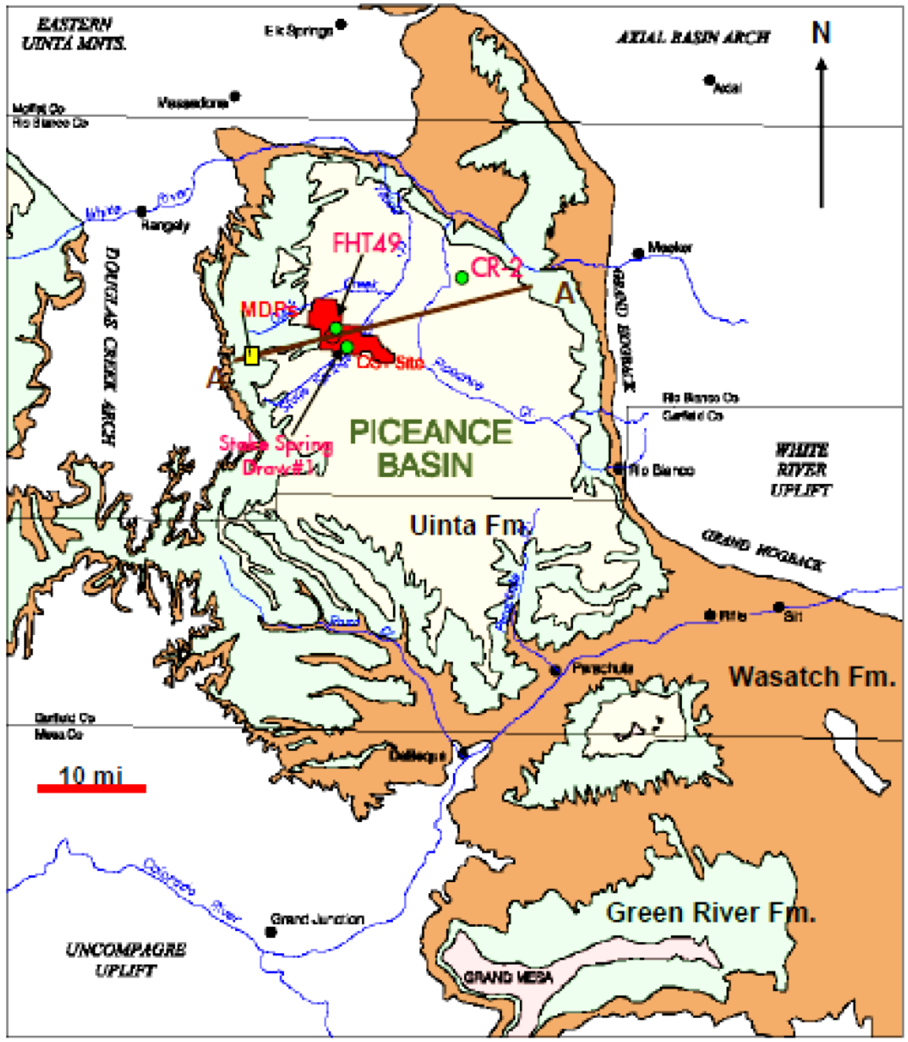


Figure 1. Geologic map of the Piceance Basin, Colorado.

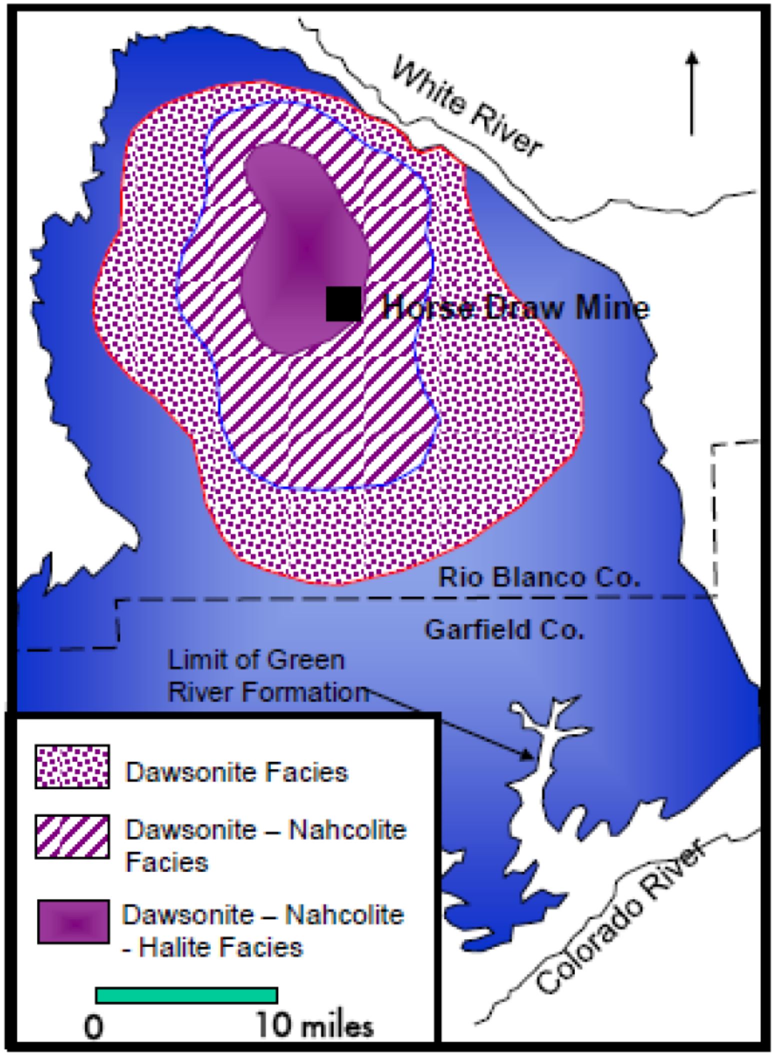


Figure 2. Map of saline mineral facies in the Northern Piceance Creek Basin (after Cole et al., 1995).

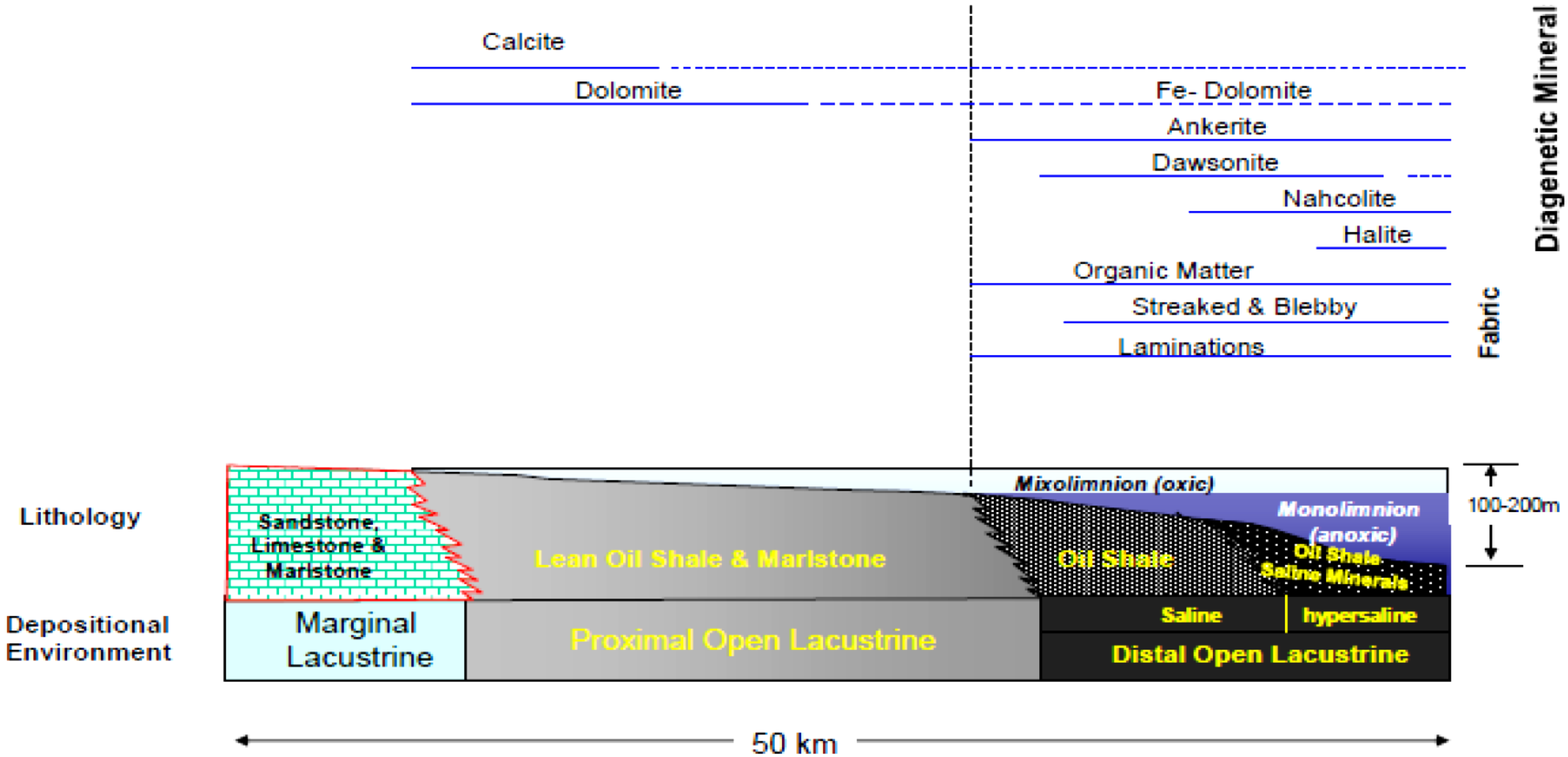


Figure 3. Diagrammatic cross section of ancient Lake Uinta in the Piceance Creek Basin during deposition of the saline zone (modified from Cole et al., 1995).

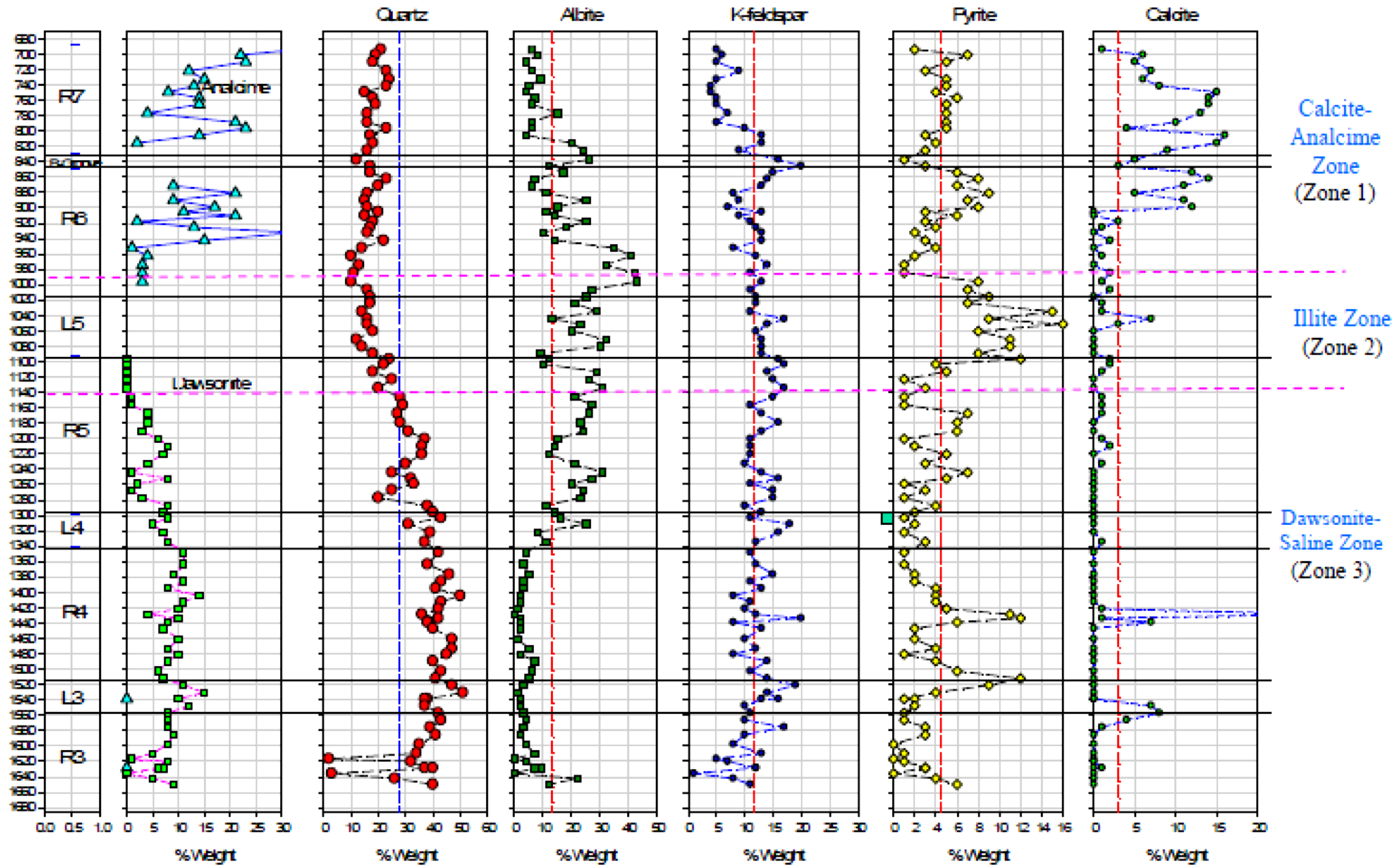


XRD Data from SURE Pyrolysis Team

Figure 4. Abundance of quartz, albite, K feldspar, pyrite, and calcite in mineral zones in the Parachute Creek Member of the Green River Formation (XRD data - FHT 49 well).

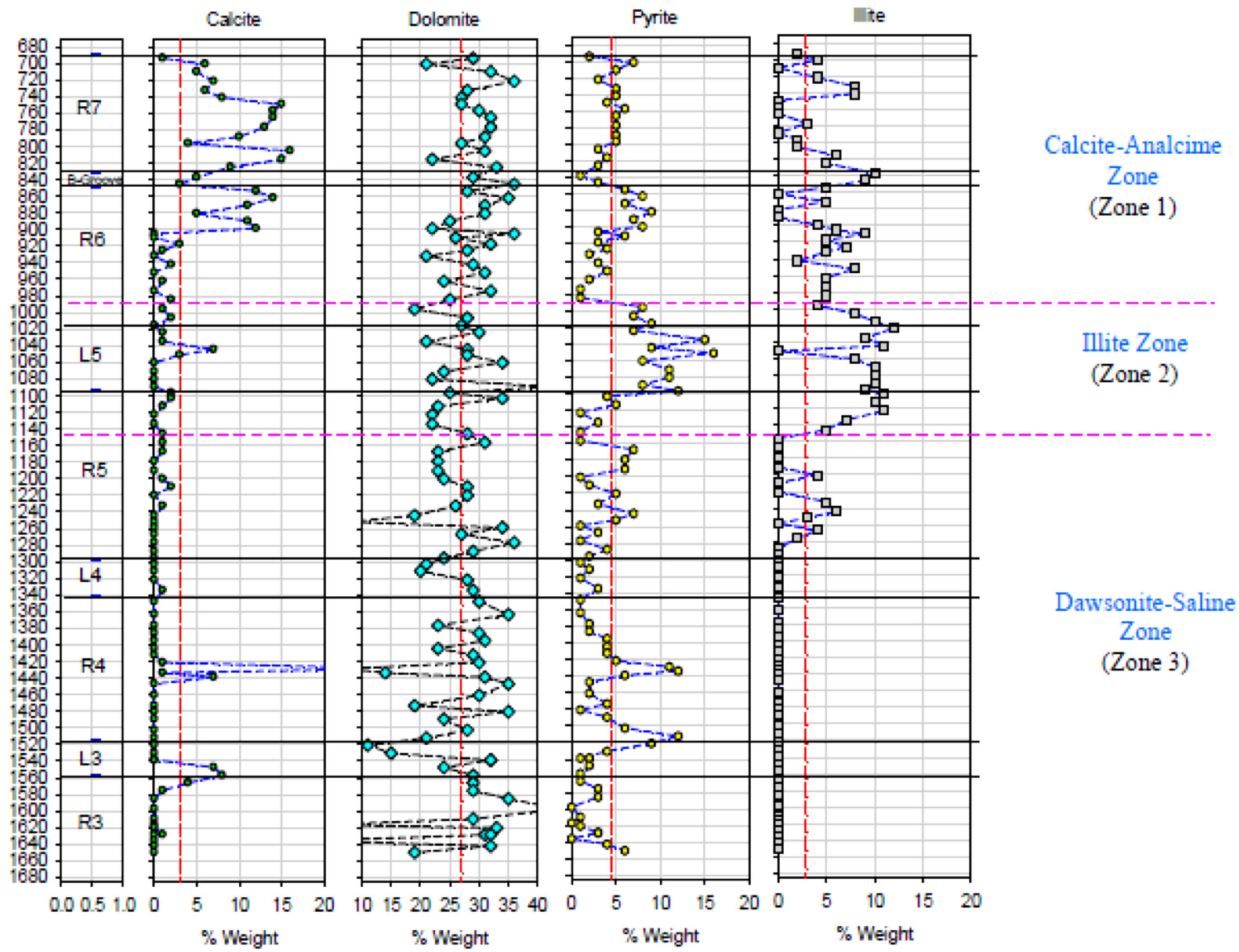


Figure 5. Abundance of calcite, dolomite, pyrite, and illite)in mineral zones in the Parachute Creek Member of the Green River Formation (XRD data - FHT 49 well).

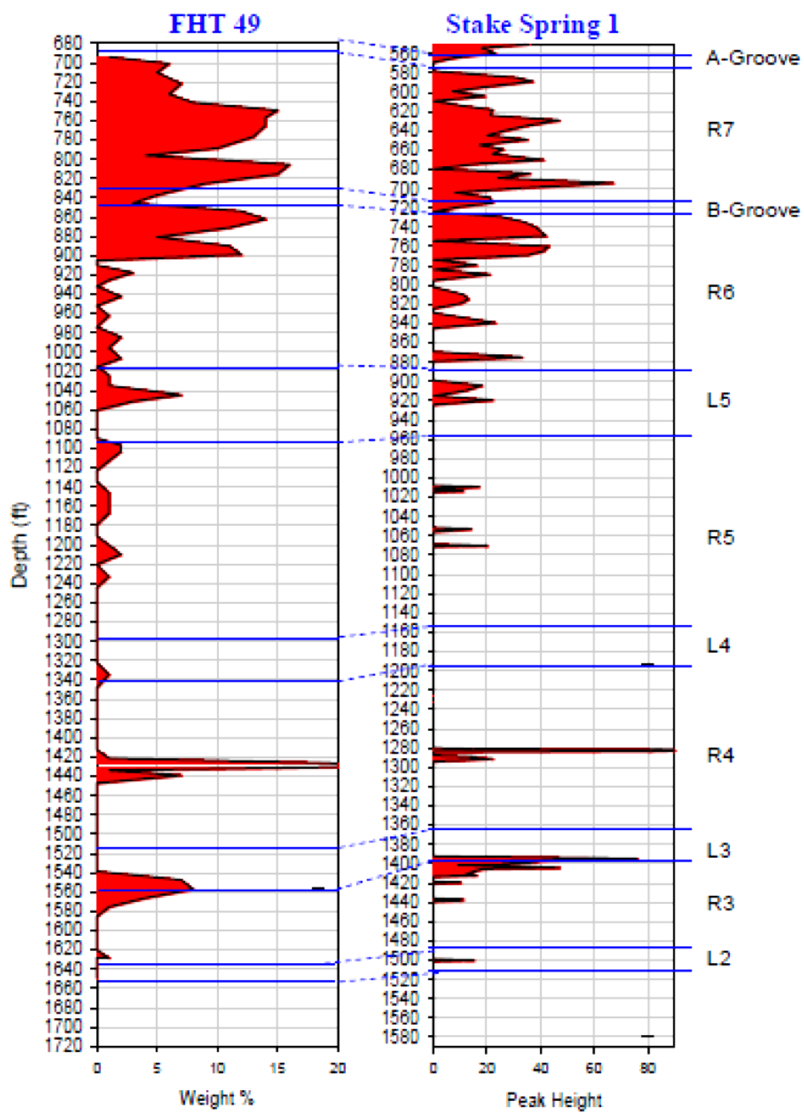


Figure 6. Calcite distribution in the FHT 49 well and Stake Spring #1 well, showing abundant calcite in the calcite-analcime zone (R7-R6) (XRD data FHT 49 well and Stake Spring well).

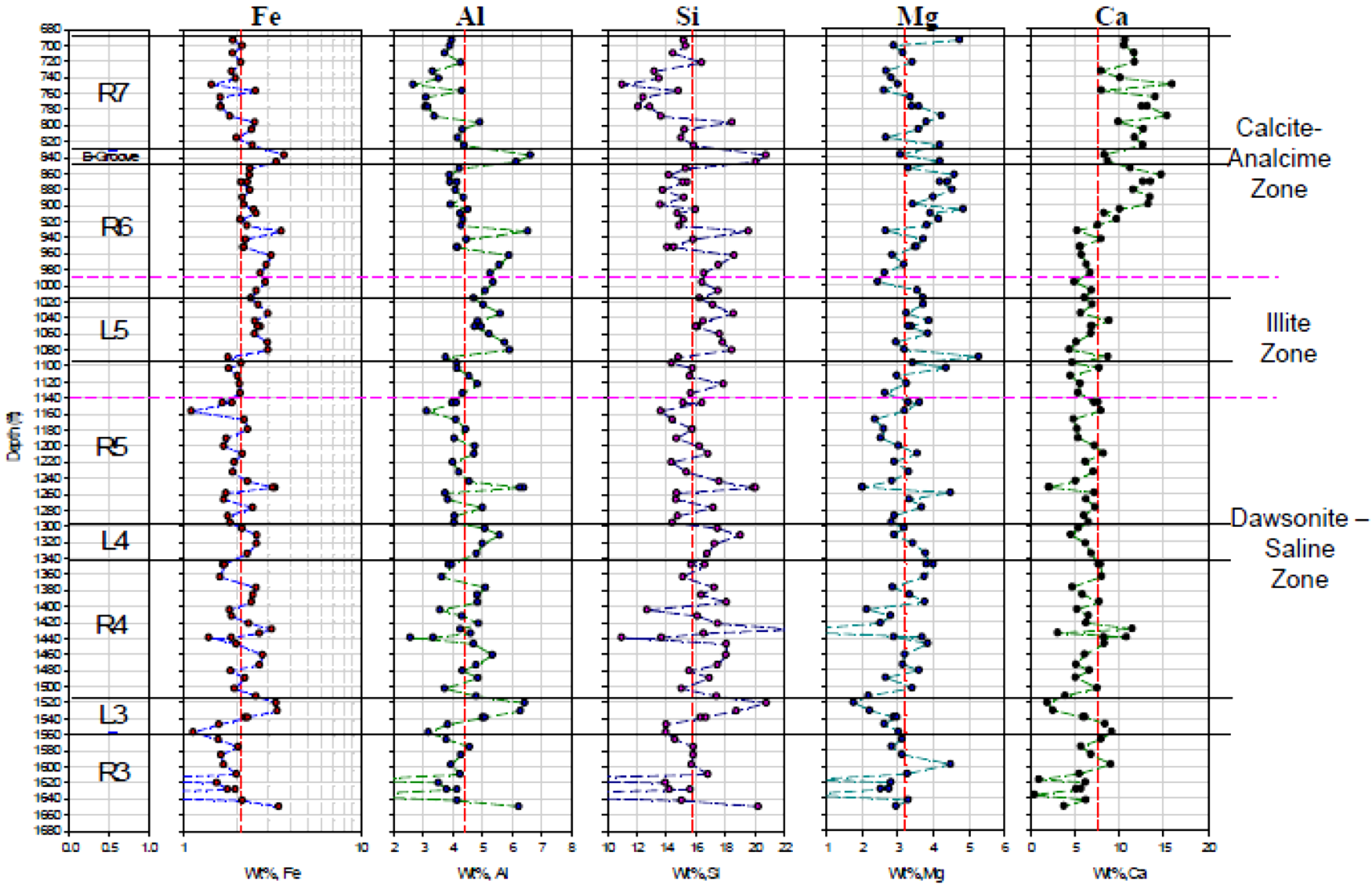


Figure 7. Abundance of major elements in the Colorado Oil Shale (FHT 49 well - 10 ft composite samples).

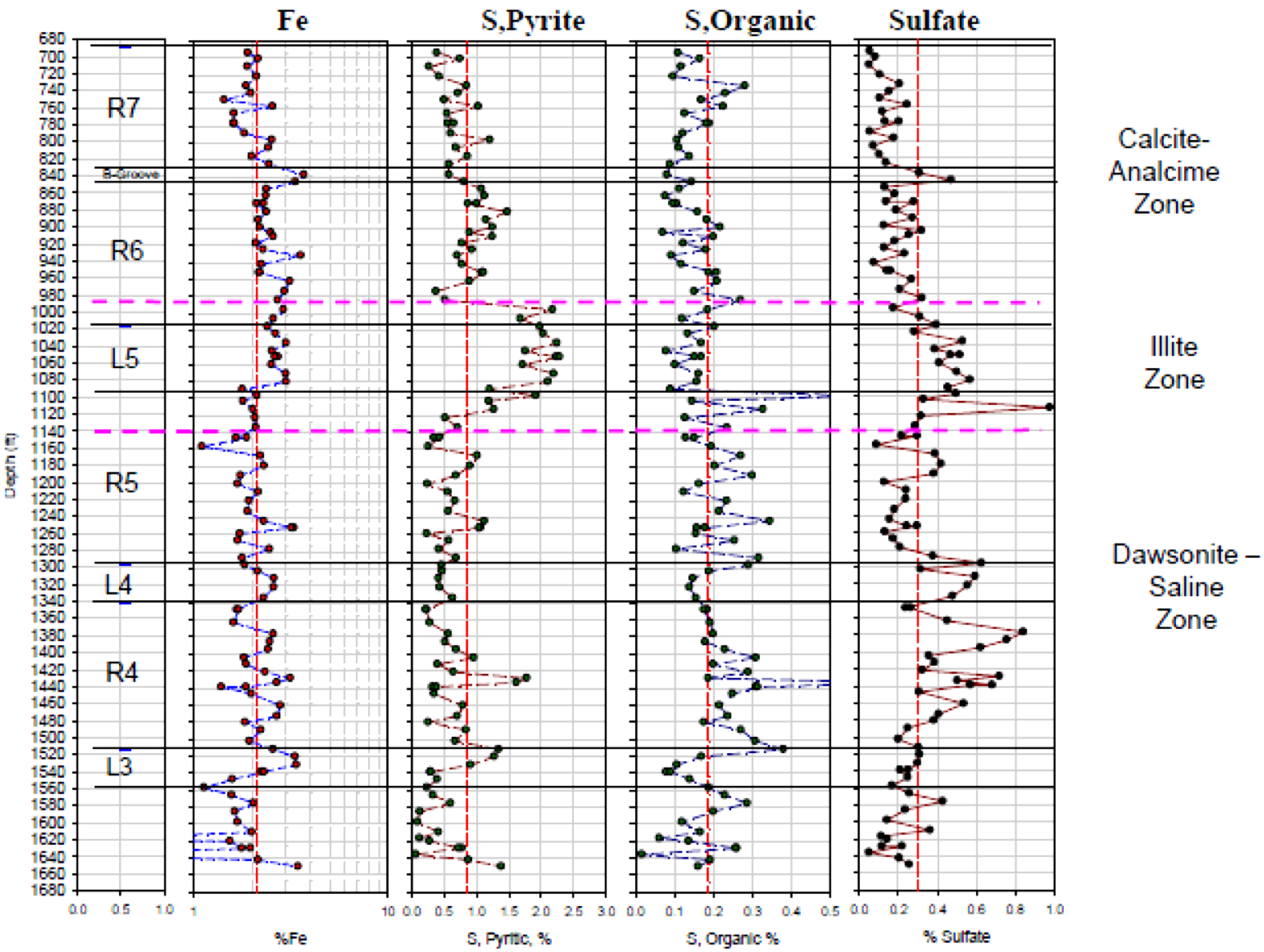


Figure 8. Abundance of iron and different types of sulfur in the Colorado Oil Shale (FHT 49 well - 10 ft composite samples).

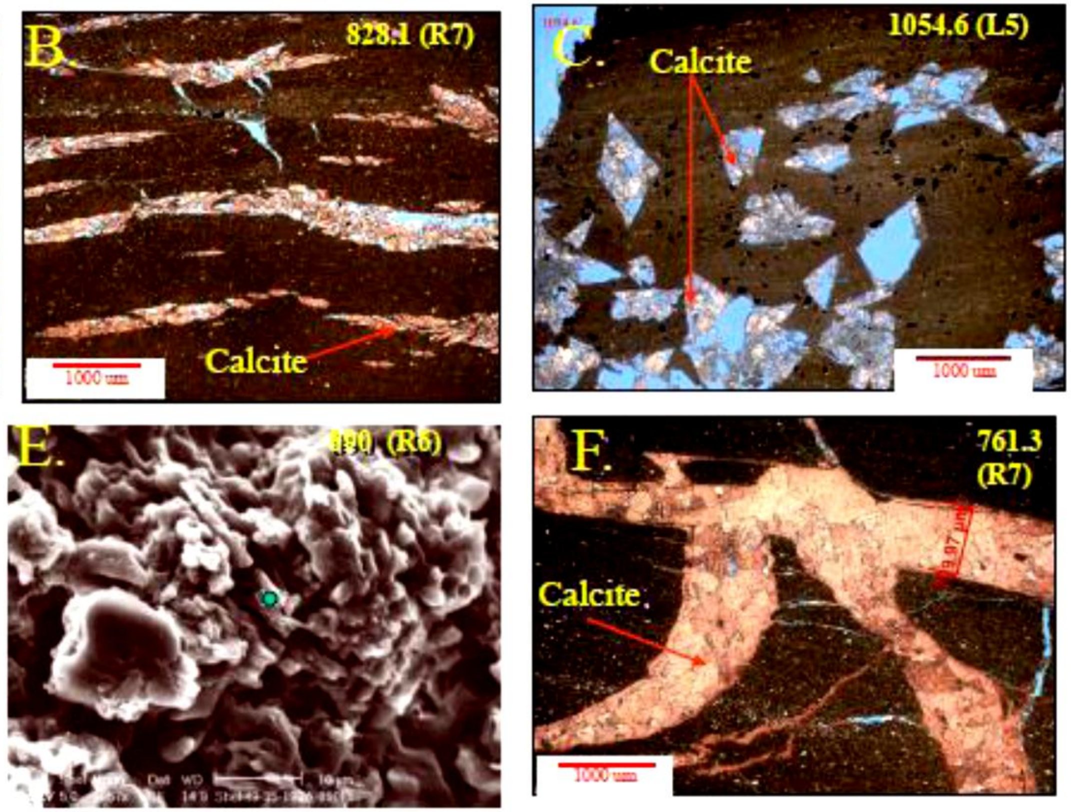


A & B. Calcite (stained red) occurs as pseudomorphs or replacing a lens-shaped evaporite mineral (possibly gypsum).
C. Calcite (stained red) partially replacing lens- to polygonal shaped evaporite mineral (possibly gypsum). This diagenetic reaction also created secondary macropores (blue epoxy).
D. Relict gypsum partially replaced by calcite (R7 Zone).
E. SEM image of a rare corroded, gypsum grain (R6 Zone). EDAX analysis (green dot) indicates: 63 wt% 0, 20 wt% Ca, and 17 wt% S. Similar remnant grains of gypsum partially replaced by calcite occur in the R3 Zone.
F. Fractures filled with calcite.

Figure 9. Occurrence of calcite and gypsum in the FHT=49 core (transmitted light photomicrographs).

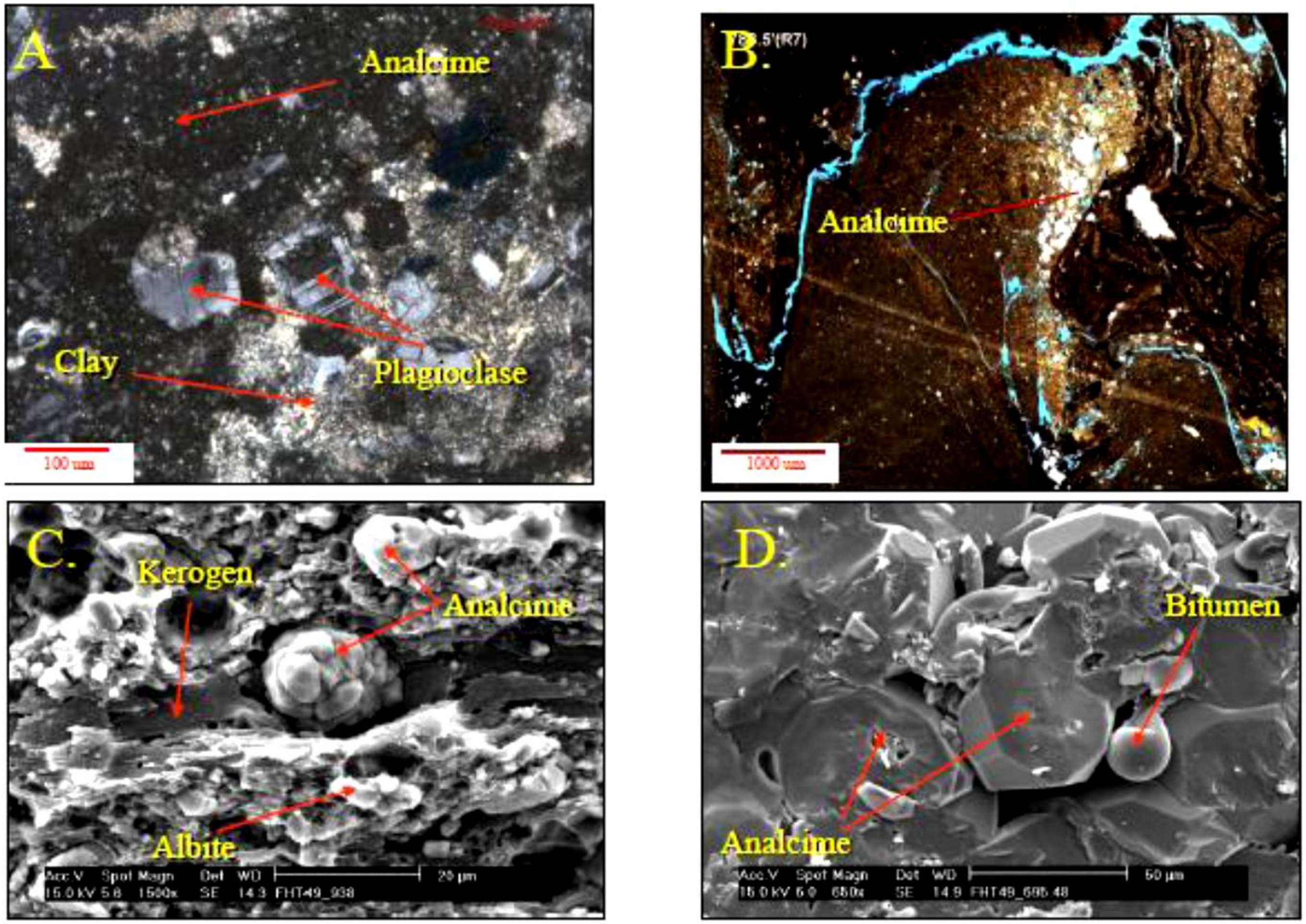


A. Sodic tuff consisting of analcime, plagioclase, and clay minerals.

B. Analcime lining a stylolite.

C. SEM image of analcime clusters embedded in oil shale matrix consisting of kerogen, fine-grained dolomite (not shown) and albite.

D. SEM image of a tuffaceous bed showing coalescing traprezohedral crystals. An intercrystalline pore is partially filled by bitumen.

Figure 10. Analcime occurrence and crystal morphology in the FHT 49 core.

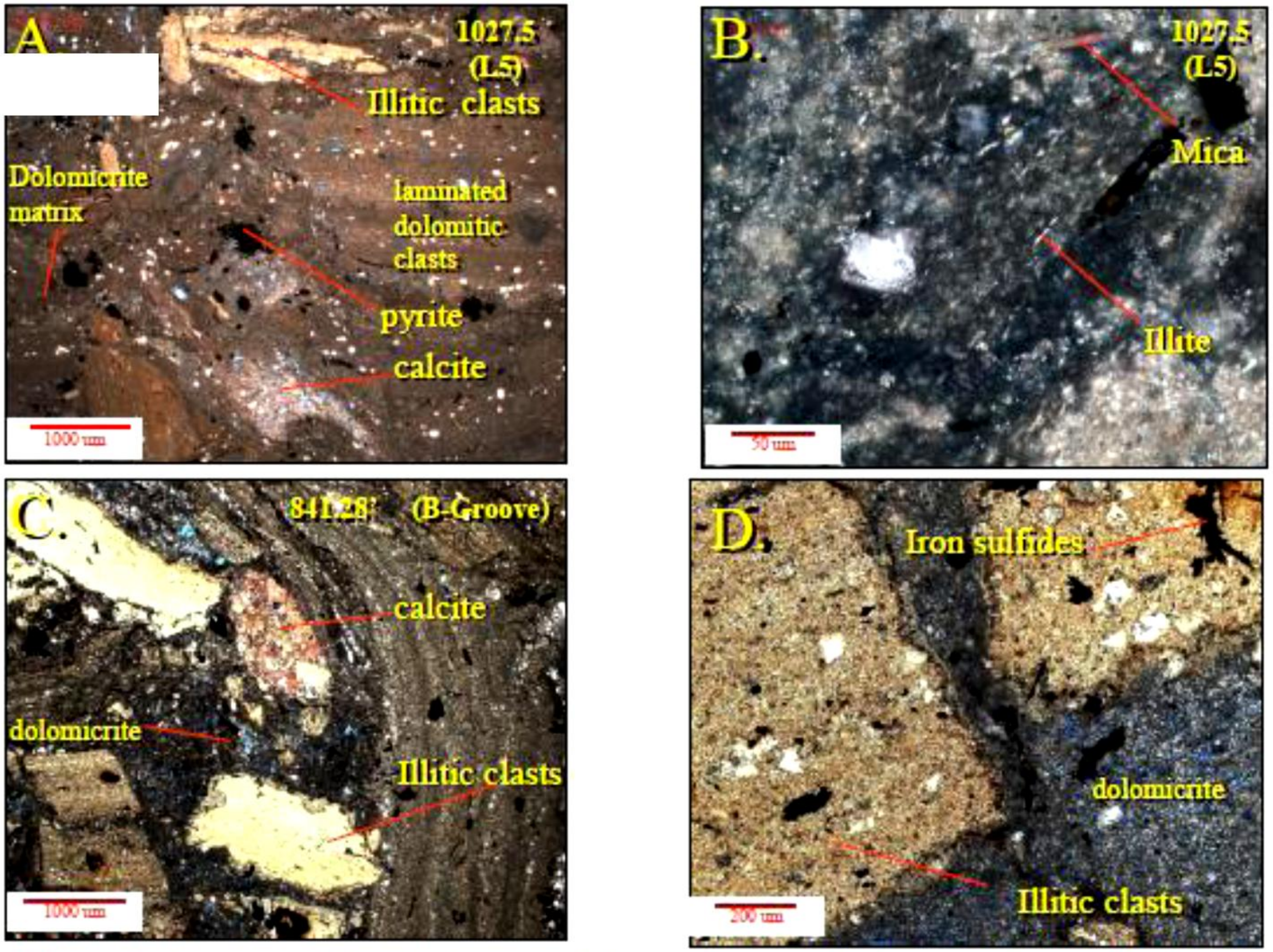


A & B Illite-rich clasts in a breccia from the L5 Zone. Plate A is a low magnification image showing illitic clasts mixed with laminated dolomitic clasts, authigenic pyrite and calcite. The supporting matrix consists of fine-grained dolomite. Plate B is a higher magnification image of an illite-rich clast (crossed nichols). The illitic clast is a mixture of detrital illite and small ($\leq 2$ μm) K-feldspar and quartz grains.

C& D Illite-rich clasts in a breccia from the B-Groove. Plate D displays illitic clasts mixed with fine-grained dolomite.

Figure 11. Occurrence of illite in the FHT 49 core (transmitted light photomicrographs).

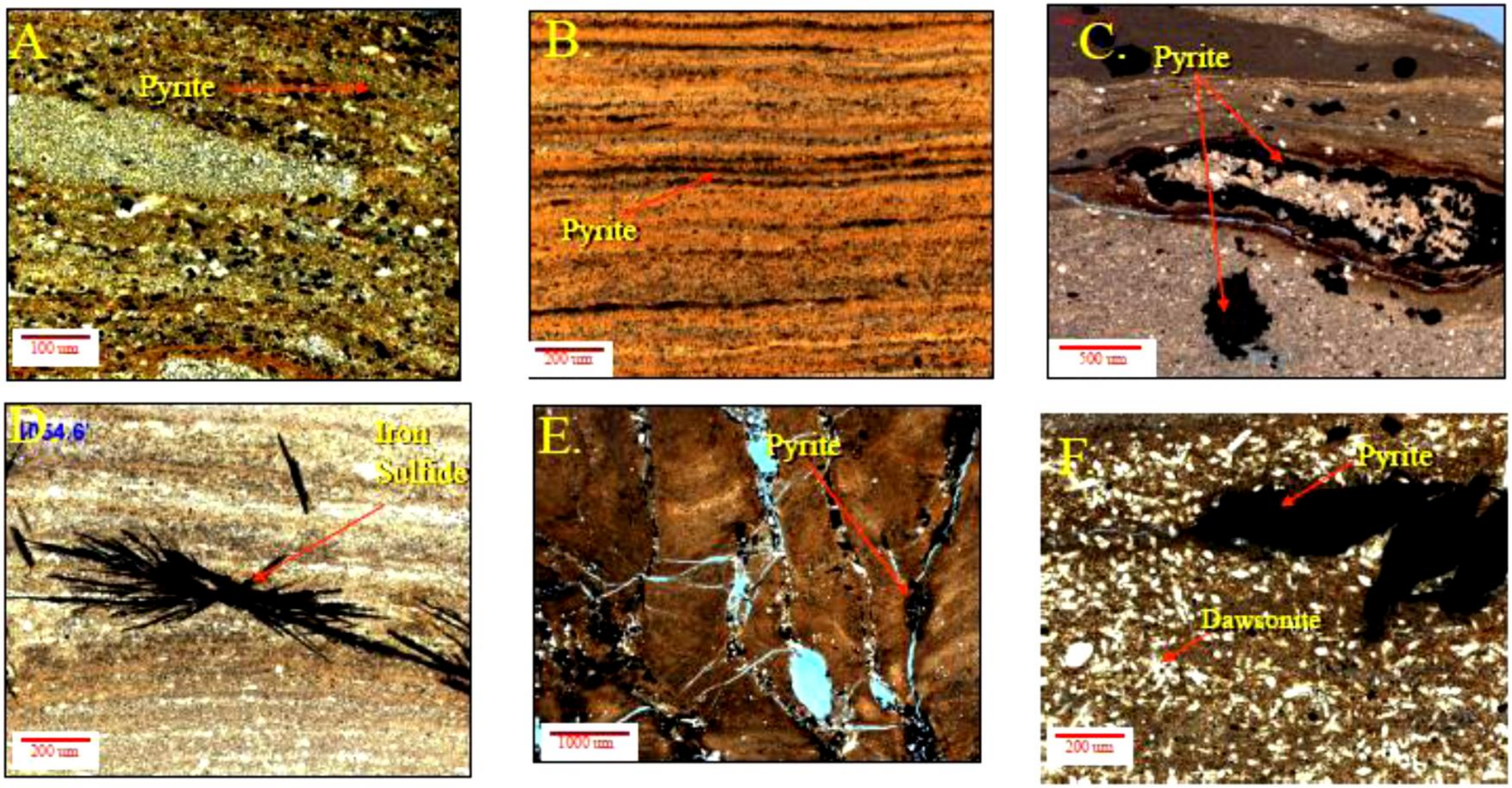


A. Small, anhedral pyrite crystals (black) dispersed in oil shale matrix.
B. Fine-grained pyrite oriented parallel to kerogen-rich laminae (brown).
C. Pyrite replacing a tuffaceous lens, and as an irregularly shaped bleb.
D. Zoned Iron sulfide blades. Pyrrhotite occurs in the center of some crystals.
E. Fracture-filling pyrite.
F. Pyrite pseudomorphs after nahcolite. Dawsonite crystals (white) also occur in organic-rich, dolomicrite matrix.

Figure 12. Occurrence of iron sulfide in the FHT 49 core (transmitted light photomicrographs).

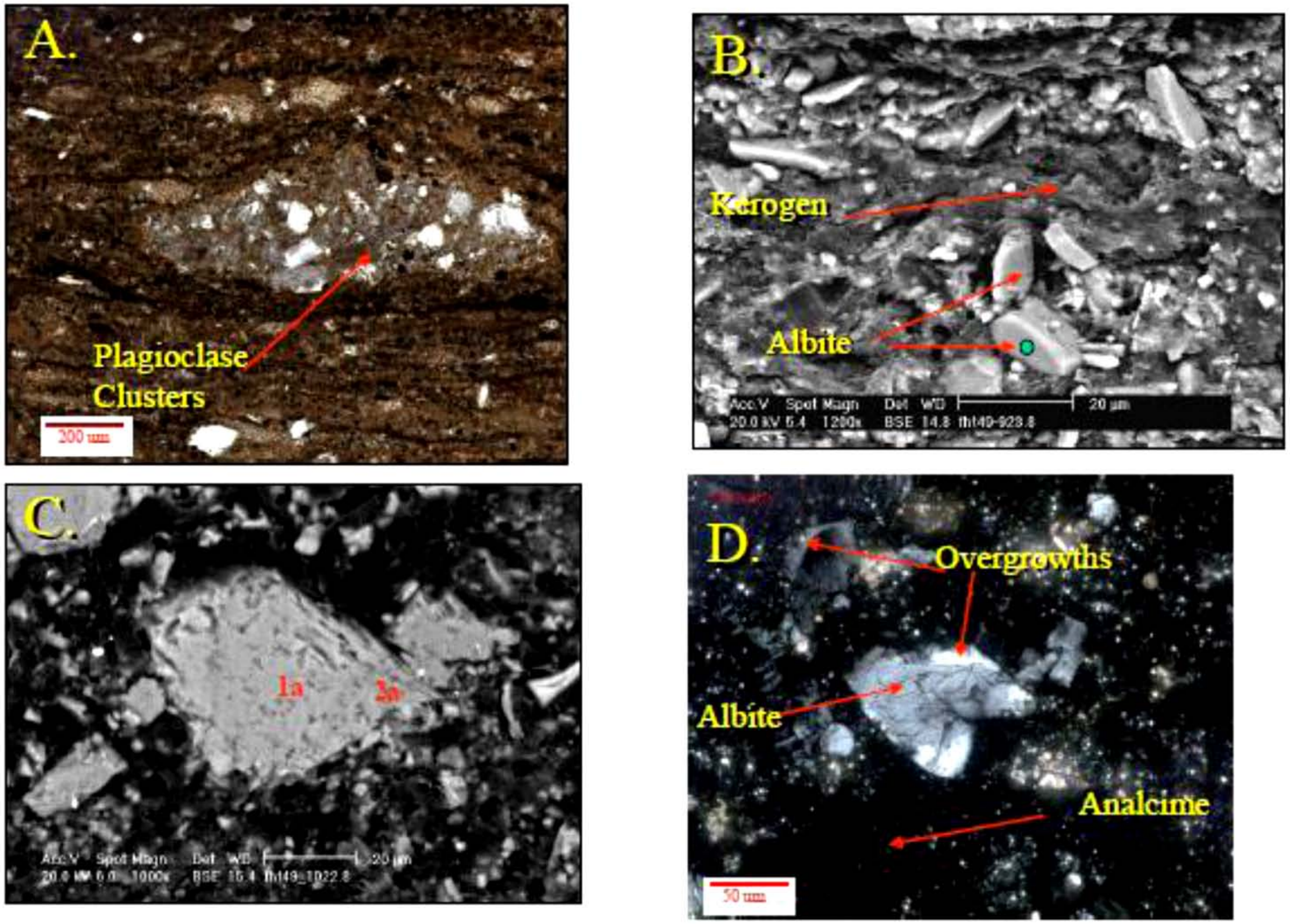


A. Clusters of plagioclase laths. Individual plagioclase grains range from 15 µm - 80 µm in length.

B. SEM image of euhedral albite crystals surrounded by a kerogen-rich matrix.

C. SEM/EDX analysis of plagioclase (1a) with albite overgrowths (2a). Plagioclase contains 41 wt% O, 7 wt% Na, 15 wt% Al, 33 wt% Si, and 5 wt% Ca. Albite composition is 39 wt% O, 9 wt% Na, 12 wt% Al, and 40 wt% Si.

D. Cross-polars photomicrograph of a tuff bed showing albite with sodic overgrowths. The isotropic mineral surrounding the plagioclase is analcime (black).

Figure 13. Plagioclase occurrence and crystal morphology in the FHT 49 core (transmitted light photomicrographs).

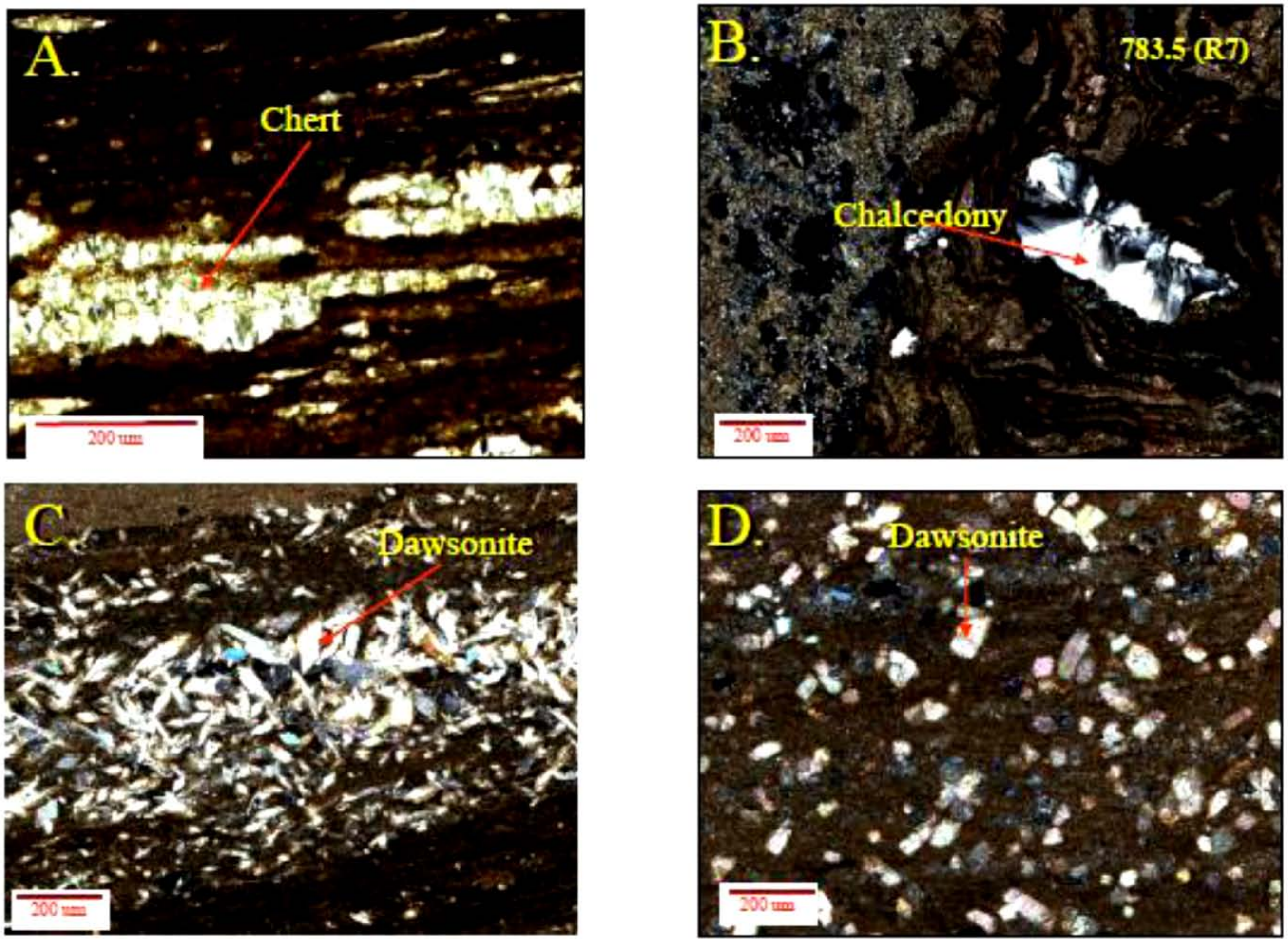


A&B Quartz occurs the form of chert (Plate A) and chalcedony (Plate B). Plate A shows lenses of microcrystalline quartz or chert. The chert lenses occur near lenses of tuffaceous material not shown in this image. Plate B shows chalcedony replacing a tuffaceous lens. Analcime is present near the chalcedony.

C&D Dawsonite crystals exhibit lath-like (Plate C) or stubby shapes (Plate D).

Figure 14. Occurrence of chert/chalcedony and dawsonite in FHT 49 core (transmitted light photomicrographs).

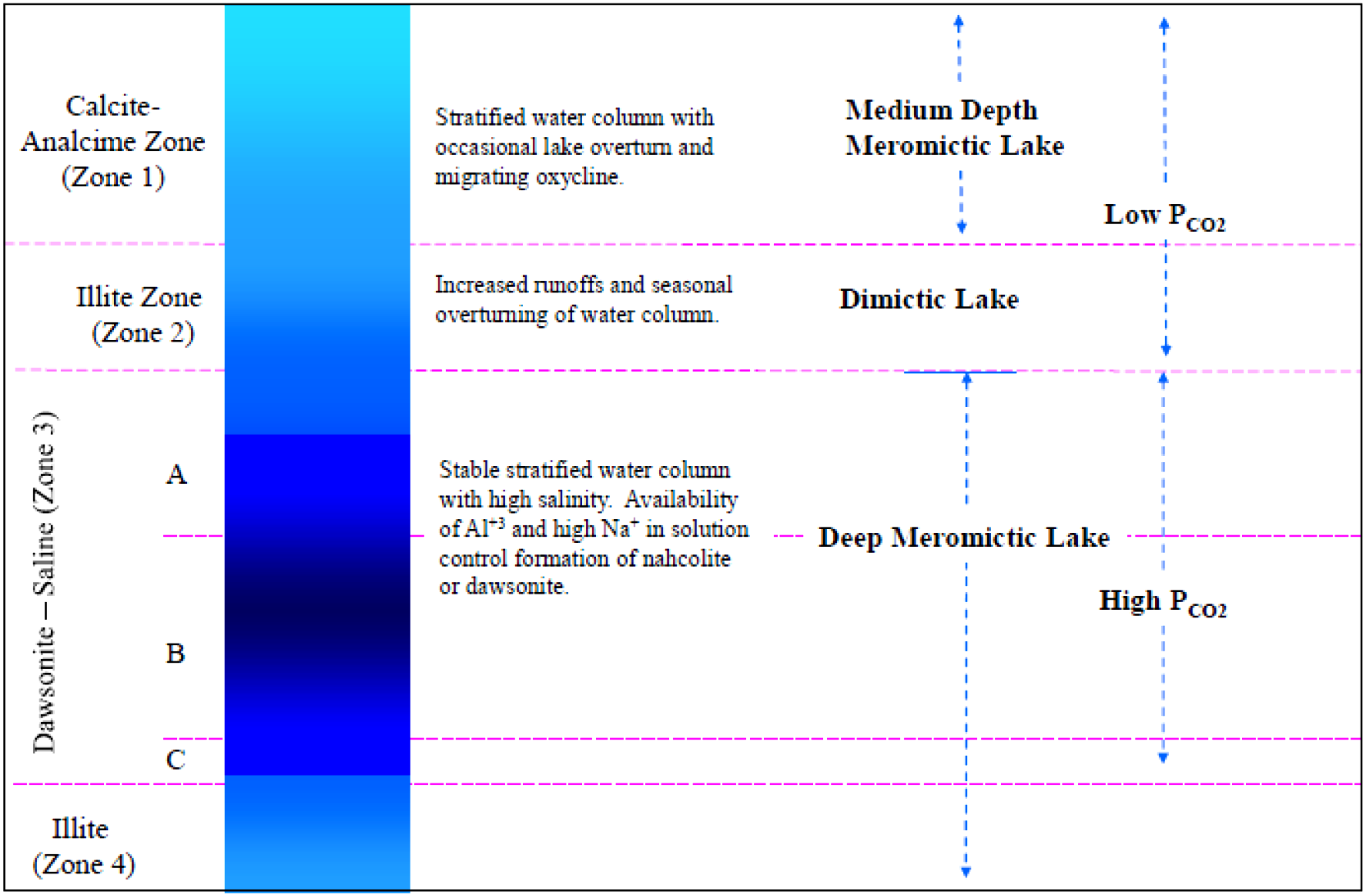


Figure 15. Paleoenvironmental interpretation of mineral zones in the Colorado Oil Shale.

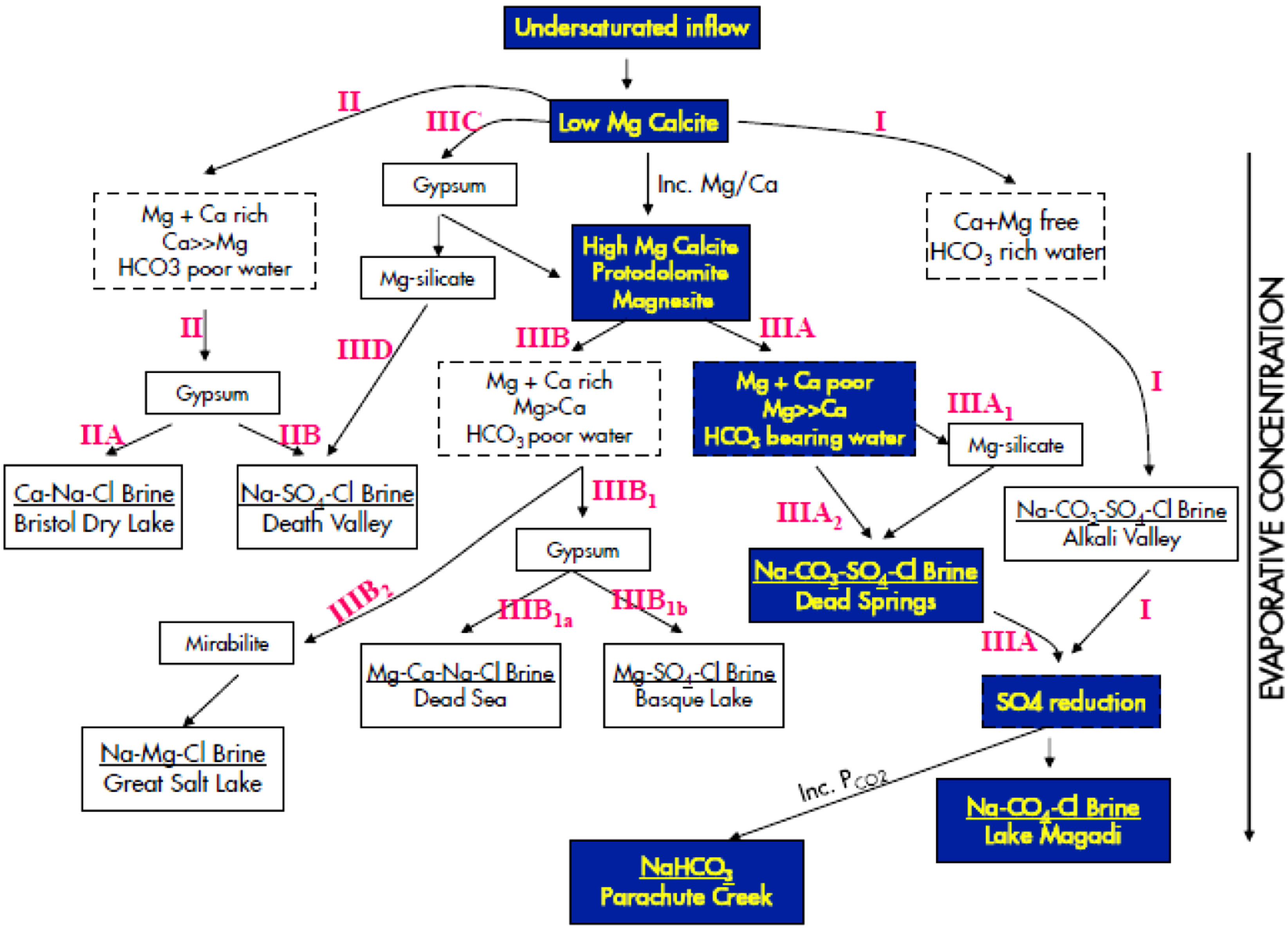


Figure 16. Brine evolution flow diagram (modified from Eugster and Hardie, 1978).

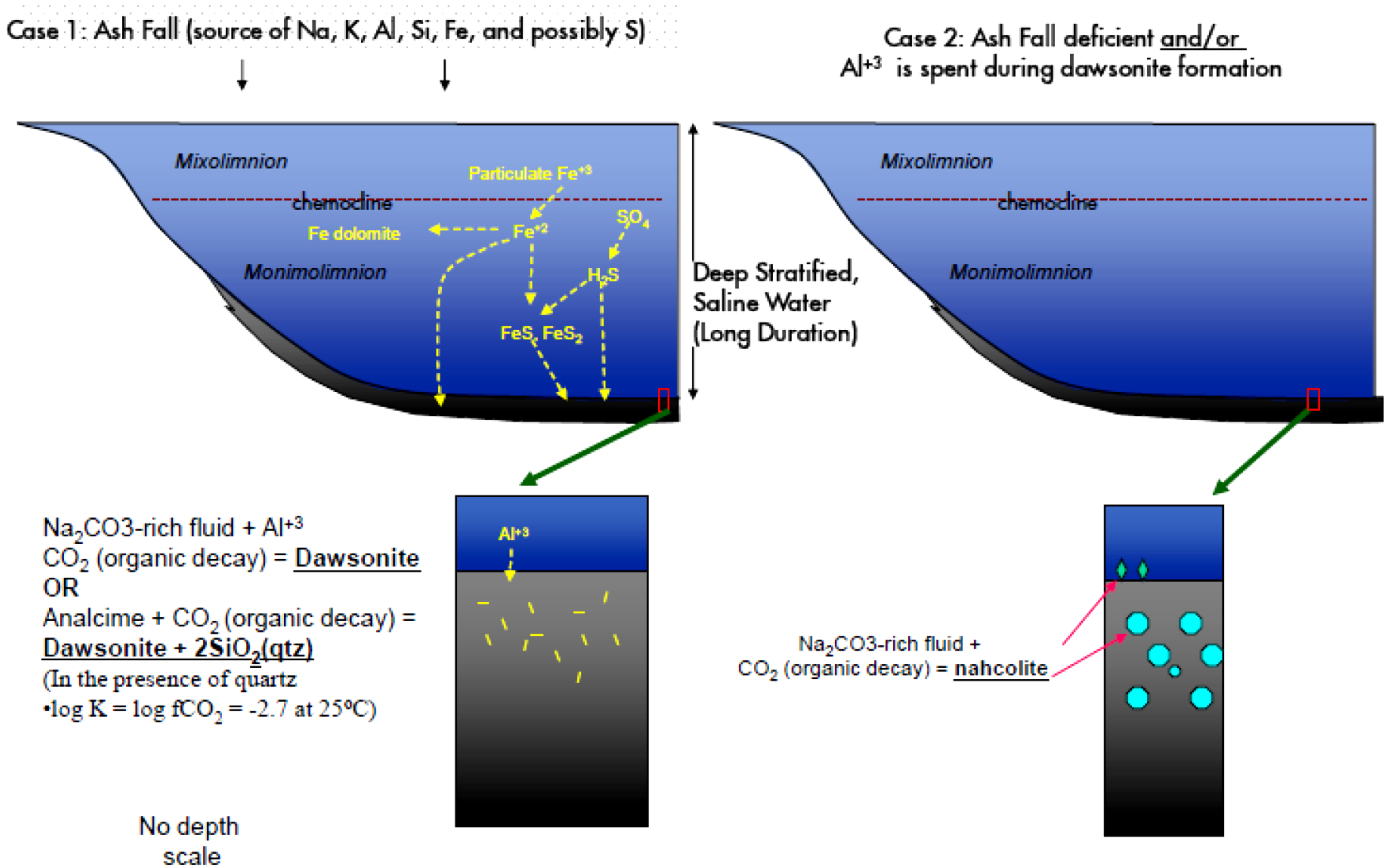


Figure 17. Depositional model during deposition of dawsonite-saline zone.

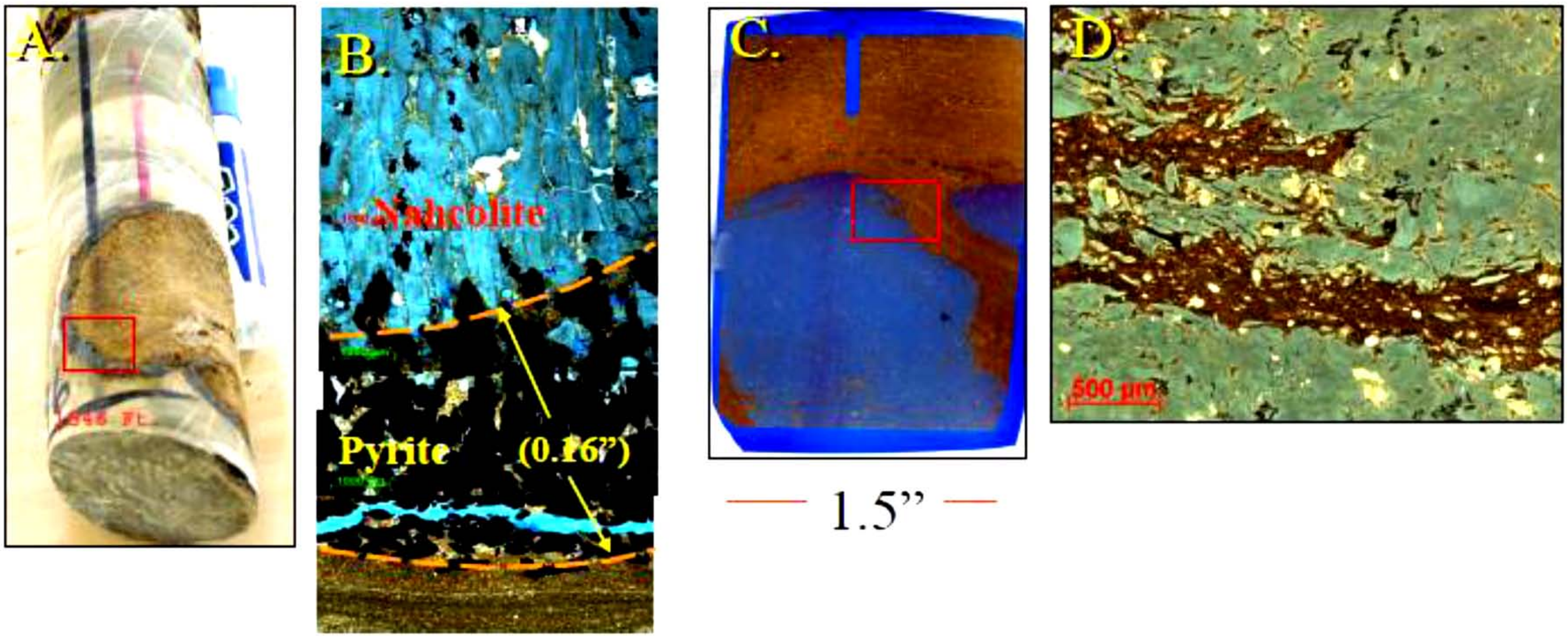


A. Large nahcolite nodule (brown) with a pyrite rim (gray) .
B. Transmitted light photomicrograph of the area outlined by the red box in plate A. The nodule consists of coalescing, lens-shaped nahcolite crystals that grew outward from the center. Pyrite psuedomorphs after nahcolite rims the nahcolite nodule.
C. Oversize thin section taken from a nahcolite aggregate.
D. Transmitted light photomicrograph of the area outlined in the red box in plate C. Individual nahcolite crystals that have coalesced enclose oil shale matrix (brown).

Figure 18. Core and microscopic views of nahcolite nodules and aggregates in the FHT 49 core.